

Alumina-Supported Cu(II), Co(II), and Fe(II) Complexes as Catalyst for Esterification of Biomass-derived Levulinic Acid with Trimethylolpropane (TMP) and Pentaerythritol (PE) and Upgrading *via* Hydrogenation

Md. Anwar Hossain,^{a,b} Cheryl Low Yi Lian,^a Md. Al-Amin A. A. Islam,^b
Md. Chanmiya Sheikh,^c Juan Joon Ching,^a and Lee Hwei Voon^a

A polyol-based ester was synthesized from biomass-derived bio-oil for application as a biolubricant. The bio-ester is biodegradable, non-toxic, and does not require mineral oil usage. Levulinic acid (LA), a major component obtained from bio-oil, was used for the catalytic esterification with two types of polyols, *i.e.*, trimethylolpropane (TMP) and pentaerythritol (PE), in the presence of alumina-supported Cu(II), Co(II), and Fe(II) complexes as catalysts. Alumina-supported Cu(II), Co(II), and Fe(II) complexes [Cu(Tyr)(GA)]Cl-alumina, [Co(Tyr)(Amp)]Cl-alumina, and [Fe(Tyr)(Amp)]Cl-alumina were synthesized by the reaction of ligands [L-tyrosine (Tyr), Gallic acid (GA), and 2-aminopyridine (Amp)] with metal chloride salts. The catalysts were characterized by elemental analyses (CHN), magnetic susceptibility, Fourier transform infrared spectroscopy (FTIR), thermogravimetric analysis/differential thermal analysis (TGA/DTA), powder X-ray diffraction (XRD), scanning electron microscopy (SEM), and energy-dispersive X-ray (EDX) techniques. Catalytic performances of the synthesized complexes were investigated *via* esterification of levulinic acid with trimethylolpropane and pentaerythritol. In addition, the two best catalysts, [Cu(Tyr)(GA)]Cl and [Co(Tyr)(Amp)]Cl-alumina, were further employed for the *in situ* hydrogenation of levulinate esters at 120 °C to 130 °C and 7 bar to 8 bar H₂ pressure for upgrading in a specially designed reactor. The alumina-supported catalysts were active, reusable, and exhibited their efficiency as heterogeneous catalysts for esterification and hydrogenation reactions for synthesizing ester-based oils.

Keywords: Biomass; Esterification; Hydrogenation; Reduced esters; Supported metal complexes

Contact information: a: Nanotechnology & Catalysis Research Centre, Institute of Postgraduate Studies, University of Malaya, Kuala Lumpur, Malaysia; b: Department of Chemistry, Rajshahi University of Engineering & Technology, Rajshahi, Bangladesh; c: Department of Applied Chemistry, University of Toyama, Toyama, Japan; *Corresponding author: leehweivoon@um.edu.my

INTRODUCTION

Sustainable and efficient biomass conversion processes are now being studied extensively to overcome the world's energy crisis for future generations (Serrano-Ruiz *et al.* 2011, 2012; Climent *et al.* 2014). The utilization of biomass as a renewable, inclusive carbon resource to produce biolubricants and useful chemicals is one of the most important alternatives for current petroleum-based technologies. Biomass (*e.g.*, wood, corn, soybean, grass, straw, algae), through pyrolysis or hydrotreating processes, are able to produce various types of organic compounds, which include biochar and bio-oil (Bridgwater 2012; Gallezot 2012). The bio-oil contains approximately 400 organic compounds, including

carboxylic acids, *e.g.*, acetic acid, levulinic acid, and propionic acid (Oliveira and da Silva 2014; Ji *et al.* 2015). Levulinic acid (LA), having five carbon atoms with carboxyl and ketone functional groups, can also be derived from glucose, fructose, starch, and lignocellulosic residues (Nandiwale and Bokade 2016). This acid has been identified by the U.S. Department of Energy as a top platform chemical, and it is regarded as one of the 12 most promising molecules derived from biomass, since it can be transformed into a variety of other important compounds in the chemical industry (Nandiwale *et al.* 2014). Levulinic acid can easily react with polyols, *e.g.*, neopentyl glycol (NPG), trimethylolpropane (TMP), and pentaerythritol (PE), in the presence of acid catalysts *via* esterification reaction to give levulinate polyol esters (Ieda *et al.* 2008). These polyol ester-base oils are used for lubricant formulation, plasticizers, fragrant chemicals, and perfumery. In this study, TMP and PE levulinate esters were synthesized, for they are expected to have analogous lubricant properties to other polyol esters, having the same viscosity index, pour point, flash point, and biodegradability. Hence, there may be wider applications for LA to produce biolubricants comparable to vegetable oils in economic perspectives.

The reduction/hydrogenation of unsaturated esters to highly stable hydrocarbon-based esters is one of the most promising reactions in organic chemistry, and therefore it is applied in a large number of chemical processes. Generally, there are two main ways to carry out such a reduction (Zhang *et al.* 2010) process. The first is the conventional hydride process, where silyl or metal hydride salts, *e.g.*, LiAlH_4 and NaBH_4 , are used, and the other is the hydrogenation process, in which molecular hydrogen (H_2) is applied. In fact, the hydrogenation reaction can be operated using small amounts of catalyst and lesser amounts/absence of solvents. Several catalysts have been used effectively in hydrogenation processes using homogeneous and heterogeneous catalytic systems, *e.g.*, alumina-supported Mn(II), Co(II), Ni(II), and Cu(II) Schiff base complexes (Salavati-Niasari and Banitaba 2003); vanadyl (IV) complexes (Salavati-Niasari *et al.* 2004), Mn(III) and Co(II) salen complexes (Chaube *et al.* 2005; Yang *et al.* 2011), and Mn(III) and Fe(III) Schiff base complexes (Adhikary *et al.* 2015).

Hydrogenation of esters using homogeneous catalysts has rarely been explored and is mostly limited to activate esters. By contrast, heterogeneous catalysts have been widely used in the hydrogenation of esters. For instance, Cu(II)-based catalysts show high activity and selectivity for hydrogenation (Yin *et al.* 2009), although the use of catalysts requires harsh reaction conditions at 200 °C to 250 °C and approximately 50 bar to 60 bar H_2 pressure. Some transition metals-based catalysts, *e.g.*, Pd, Ru, Pt, Rh, and Re, are also analyzed to be useful for the hydrogenation of esters.

The application of transition metal complexes has received great attention from modern researchers in the last few years due to their ability to act as a catalyst or catalyst precursor. The thermal stability and tenability of mixed ligand complexes make them truly suitable for a wide range of catalytic and stoichiometric transformations. These comprise many reactions, including bond activation (Choi *et al.* 2009; Huang *et al.* 2009), carbon-carbon bond formation (Goldman *et al.* 2006; Castonguay *et al.* 2008), polymerization (Müller *et al.* 2002), conversion of ammonia from nitrogen and hydrogen (Arashiba *et al.* 2011), organic synthesis (Chakraborty *et al.* 2009), and supramolecular chemistry (Morales-Morales and Jensen 2007).

The simplest approach to transform a homogeneous catalyst into a heterogeneous catalytic system comprises of immobilization or encapsulation of active metal complexes onto a solid support. The grafting of well-defined soluble homogeneous organometallic

catalysts onto a suitable insoluble inorganic solid support has been demonstrated to be a promising and stable method for recycling (Swennenhuis *et al.* 2009; Abbott *et al.* 2014; Karakhanov *et al.* 2014; Goni *et al.* 2017).

Encapsulation eases separation of metal complex catalysts by simple filtration. In addition, the impregnation method enhances catalyst stability and selectivity (Karakhanov *et al.* 2014) towards organic reactions. Many useful methods have been adopted for grafting of metal complexes onto solid support, including ion pairing and encapsulation (Jones *et al.* 2005), physisorption, and covalent ligand binding. However, immobilization of metal complexes by covalent attachment onto a solid support gives the best recovery process for homogeneous catalysts (del Pozo *et al.* 2010).

Current studies have revealed the methods of immobilizing metal complexes on a solid support, including inorganic materials (*e.g.*, silica, alumina, silica-alumina, SBA-15, MCM-41, MCM-48) and functionalized organic polymers (Bergbreiter *et al.* 2001; Chase *et al.* 2004). Porous alumina support materials seem to be most useful and versatile solids for immobilization of organometallic complexes (Mehendale *et al.* 2007). Under these backgrounds, the authors have chosen acidic alumina as support material because neither neutral nor basic alumina are able to adsorb the metal complexes on its surface uniformly. More importantly, the adsorbing tendency of alumina might arise from the presence of oxygen on its structures (Salavati-Niasari *et al.* 2004), which can coordinate to the metal ion (Fig. 1). Indeed, this mesoporous structural integrity enhances the uniform loading of organometallic complexes onto the supports and facilitates catalytic activity of reaction substrates.

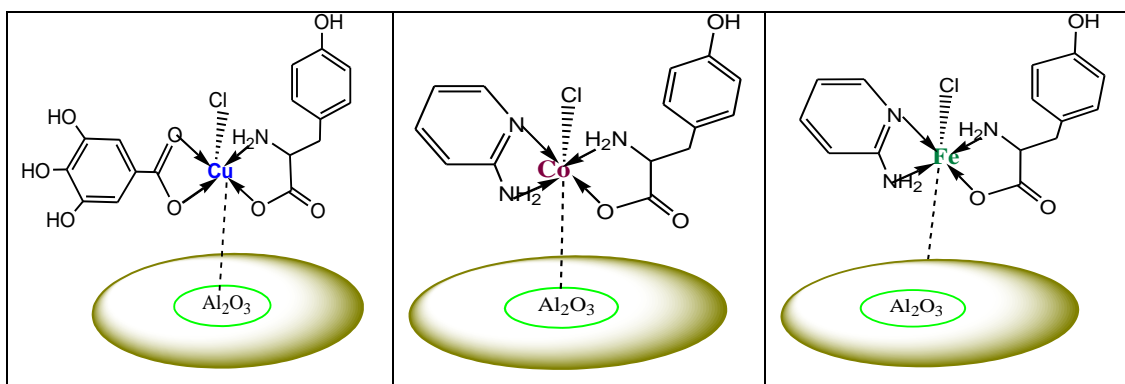


Fig. 1. The probable structure of metal complexes grafted by alumina support

It is well known that 3rd row transition metals are cheaper than Pd, Pt, Rh, and Ru, and their complexes are widely used for the hydrogenation of organic compounds. The physicochemical properties of these complexes are characterized using various techniques. However, the two potential catalysts are used for the hydrogenation of levulinate ester to corresponding reduced esters.

Herein, the authors report the full detailed synthesis of [Cu(Tyr)(GA)]Cl-alumina, [Co(Tyr)(Amp)]Cl-alumina, and [Fe(Tyr)(Amp)]Cl-alumina catalysts. Their catalytic performance is studied *via* esterification reaction of levulinic acid (LA) with trimethylolpropane (TMP) and pentaerythritol (PE), respectively. Notably, the proposed hydrogenation reaction pathways for levulinate ester over Cu complex and alumina-supported Co-based catalysts are also investigated.

EXPERIMENTAL

Materials

All the chemicals and solvents were of analytical grade and used without further purification. L-tyrosine was obtained from Sigma-Aldrich (St. Louis, MO, USA), while gallic acid and 2-aminopyridine were purchased from Merck (Mumbai, India). The metal salt Cu(II), Co(II), and Fe(II) chlorides were received from Fluka Chemica (Buchs, Switzerland). Acidic alumina was also purchased from Merck and activated by calcination at 450 °C for 8 h before use. For catalytic reactions levulinic acid and polyols *e.g.*, trimethylolpropane (TMP) and pentaerythritol (PE), were also obtained from Merck.

Physical Measurements

Fourier-transform infrared spectroscopy (FTIR) analyses were scanned at the range of 4000 cm^{-1} to 400 cm^{-1} with pressed KBr pellets using an IR-8400/8900 Shimadzu spectrophotometer (Kyoto, Japan). Magnetic susceptibility measurements were carried out using a magnetic susceptibility balance (Sherwood Scientific, Cambridge, UK). The elemental analysis (carbon, hydrogen, and nitrogen) and metals were recorded by using a Yanaco CHN-corder-MT-5.

The physical structure of catalysts, compositional analysis, and surface morphology observation were measured by scanning electron microscopy (SEM) (JEOL, JSM-6360 LV, Tokyo, Japan) coupled with energy-dispersive x-ray spectroscopy (EDS) (JEOL, JED-2300). The thermal decomposition behavior of residual hydrocarbons on the spent catalysts was performed using thermogravimetric and differential thermal analysis (TGA/DTA 60, Shimadzu) at a heating rate of 10 °C/min from room temperature to 800 °C under nitrogen flow.

Powder x-ray diffraction (XRD) analysis was performed using Rigaku RINT 2200 equipment (Tokyo, Japan) with Cu-K α radiation operated at 40 kV and 40 mA. Data were collected over a 2θ range of 10 ° to 90°, and phases were identified by matching experimental patterns to entries in the Version 6.0 indexing HighScore Plus software (Kottrak, London, UK).

Synthesis of Metal Complexes

The syntheses of complexes followed the following reaction pathways shown in Fig. 2. The reaction with Al₂O₃ at 40 °C to 50 °C for 8 h gave the following supported complexes: alumina-supported Cu(II), Co(II), and Fe(II) complexes (Fig. 1).

Preparation of [Cu(Tyr)(GA)]Cl-Al₂O₃

This complex was prepared with a water:methanol (1:3) solution of gallic acid (Taha *et al.* 2016) (1 mmol) and L-tyrosine (1 mmol) that was previously prepared *via* deprotonation by alkali (NaOH, 0.05 mmol), to the copper(II) chloride solution (1 mmol) in methanol-water solution, and continuously stirred at 70 °C to 80 °C for 2 h. Upon cooling the solution, a blue powdered compound obtained was filtered, washed with methanol, dried under vacuum condition, and purified by recrystallization from ethanol. Selected IR data (KBr pellet, cm^{-1}): 3334, 3324, 3146, 2945, 1594, 1571, 1448, 1358, 1349, 1245, 1056, 532, and 496. Magnetic susceptibility; $\mu_{\text{eff}} = 1.81$ (Paramagnetic).

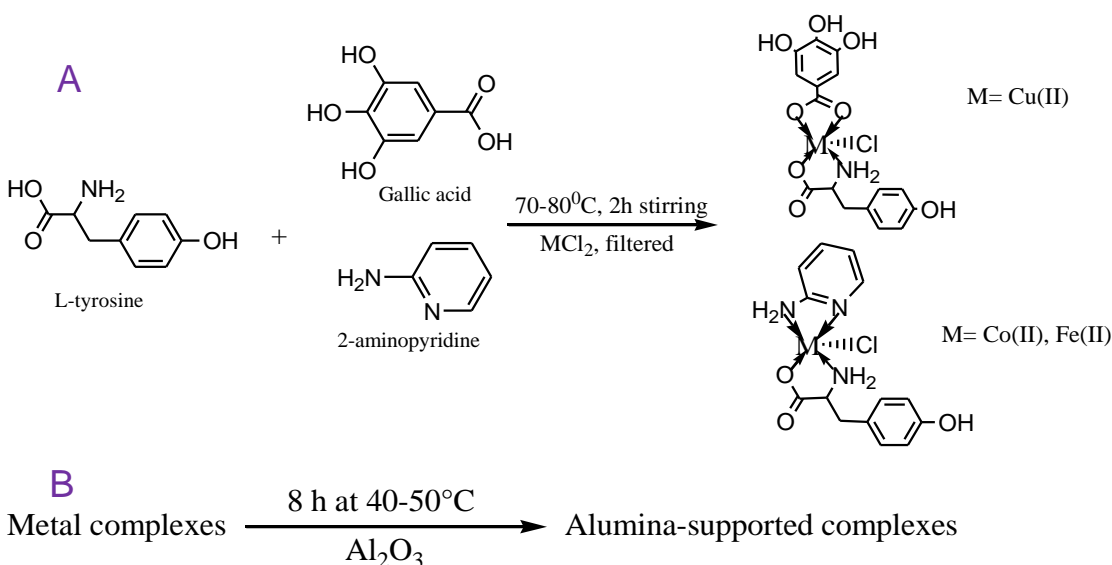


Fig. 2. Synthetic route of preparing metal complexes using L-tyrosine, gallic acid, and 2-aminopyridine ligands (A), and Al_2O_3 supported complexes (B)

A solution of the $[Cu(Tyr)(GA)]Cl$ in CH_3OH was added to a suspension of Al_2O_3 in methanol at a ratio of 1:6. The resulting suspension was stirred at $40^\circ C$ to $50^\circ C$ for 8 h. The blue solid was filtered, and then it was washed with methanol. The $[Cu(Tyr)(GA)]Cl-Al_2O_3$ catalyst was dried at $60^\circ C$ under vacuum overnight prior to use. Selected IR data (KBr pellet, cm^{-1}): 3504, 3134, 2845, 1584, 1573, 1445, 1355, 1351, 1252, 1058, 529, and 493.

Preparation of $[Co(Tyr)(Amp)]Cl-Al_2O_3$

The same procedure for the preparation of $[Cu(Tyr)(GA)]Cl-Al_2O_3$ was repeated by substituting gallic acid ligands with 2-amino pyridine and Cu(II) metal center with Co(II). The violet solid was obtained on slow evaporation of the concentrated solution. Selected IR data (KBr pellet, cm^{-1}): 3348, 3157, 3131, 2942, 1605, 1568, 1441, 1353, 1353, 1236, 1080, 545, and 487. Magnetic susceptibility; $\mu_{eff} = 4.26$ (paramagnetic).

Alumina powder was added to a solution of $[Co(Tyr)(Amp)]Cl$ in methanol (1:6) and heated at $40^\circ C$ to $50^\circ C$ for 8 h with constant stirring. The solid was filtered, washed with methanol, and dried at $60^\circ C$. Selected IR data (KBr pellet, cm^{-1}): 3503, 3135, 2941, 1603, 1565, 1351, 1234, 1080, 548, and 485.

Preparation of $[Fe(Tyr)(Amp)]Cl-Al_2O_3$

The method for synthesizing $[Co(Tyr)(Amp)]Cl-Al_2O_3$ was repeated by substituting Co(II) metal salt with Fe(II) (Jana *et al.* 2009; Santoro *et al.* 2015). The green solid obtained on slow evaporation of concentrated solution was suitable for powder x-ray diffraction. Selected IR data (KBr pellet, cm^{-1}): 3324, 3146, 2945, 1594, 1571, 1358, 1448, 1349, 1245, 1056, 532, and 496. Magnetic susceptibility; $\mu_{eff} = 3.65$ (Diamagnetic) (Santoro *et al.* 2015).

Porous alumina was added to the solution of $[Fe(Tyr)(Amp)]Cl$ in methanol (1:6) and heated at $40^\circ C$ to $50^\circ C$ for 8 h with constant stirring. The solid compound was filtered, washed with methanol, and dried at $60^\circ C$. Selected IR data (KBr pellet, cm^{-1}): 3505, 3324, 2948, 1592, 1573, 1450, 1032, 535, and 491.

Catalytic Activity Experiments

Esterification

The catalytic activity experiments were conducted *via* esterification of levulinic acid (LA) with polyols (*i.e.*, TMP and PE) under reflux condition at reaction temperature of 110 °C to 130 °C in a silicone oil bath with continuous magnetic stirring. The activities of catalysts were measured by varying different parameters involved (*e.g.*, reaction time, % of catalyst loading, and polyols to LA molar ratios). Prior to reaction, the complex catalysts were dried at 70 °C to 80 °C for 6 h. Preliminary studies using sulfuric acid as a homogeneous catalyst were performed in an esterification reaction to estimate the range of reaction conditions. Blank experiments were carried out to validate the activity of the catalyst complexes. The applied reaction conditions were such that there was no external mass transfer; hence, the experiments were conducted under the same kinetic regime. After completion of reaction, the products were collected and analyzed by Gas Chromatography-Mass Spectrometer (GC-MS, Shimadzu-QP 5000) equipped with RTX-5-MS column (30 m × 0.25 mm × 0.25 μm) in split mode. The fraction peaks obtained from mass spectra were identified using the National Institute of Standards and Testing (NIST) library matching. Further, catalytic activity of the catalysts towards esterification (total product yield and product selectivity) was determined by comparing the peak area % of obtained spectra. It is known that the GC-MS analyses do not provide exact quantitative analytical results of compounds. However, it is possible to compare the product yield and selectivity by comparing the peak areas since the chromatographic peak area of compounds is proportional to its quantity and the relative content of the product (Eqs. 1 and 2) (El Khatib *et al.* 2015; Yi Lian *et al.* 2017). In order to confirm the reproducibility of the results, the experiments were performed three times, where the average of the peak area and peak area % was calculated.

$$\text{Product Yield (\%)} = \frac{\text{Total area of product} - \text{area of reactant}}{\text{Total area of product}} \times 100\% \quad (1)$$

$$\text{Product Selectivity (\%)} = \frac{\text{Area of desired product}}{\text{Total area of product}} \times 100\% \quad (2)$$

Hydrogenation

Hydrogenation of TMP and PE-levulinate esters was carried out using a closed system pressure reactor with mechanical stirring. The reactor was initially purged with nitrogen gas flow for 3 min to 5 min to eliminate any traces of oxygen in the system. Approximately of 7 bar to 8 bar of hydrogen was then introduced to the reactor before the reaction began. The reaction temperature was set at 120 °C to 130 °C with a heating rate of 10 °C/min and holding time of 2 h. The stirring speed was maintained around 120 rpm to 130 rpm. At the end of reaction time, the reactor was cooled and the gases were liberated. The reduced ester products were collected and sent for gas chromatography mass spectrometry (GC-MS) and FT-IR analysis.

RESULTS AND DISCUSSION

The complexes [Cu(Tyr)(GA)]Cl-alumina, [Co(Tyr)(Amp)]Cl-alumina, and [Fe(Tyr)(Amp)]Cl-alumina were successfully synthesized for the first time by reacting Cu(II), Co(II), and Fe(II) chlorides with aromatic bidentate ligands L-tyrosine, 2-aminopyridine, and gallic acid as mixed ligands in water-methanol solution at 70 °C to 80 °C. Afterwards, the complexes were impregnated with solid inorganic supports (alumina)

to prepare the tethered complexes. The thermal stability, magnetic susceptibility, and spectroscopic and X-ray diffraction studies were described in the Experimental section. All the analytical and spectroscopic features were consistent with six coordinated complexes in all the cases, and they were insoluble to the common organic solvents. The relevant IR spectroscopic and GC-MS analysis for ester products were interpreted herein.

IR Spectra Analysis

The solid-state IR spectra of the ligand metal complexes with or without immobilization on alumina were in the range of 4000 cm^{-1} to 400 cm^{-1} (Figs. 3A, 3B, and 3C). Absorption peaks at 2930 cm^{-1} to 2870 cm^{-1} were attributed to C-H stretching vibrations in methylene ($-\text{CH}_2-$) groups (Dholariya *et al.* 2013) of the complexes, while in impregnated molecules, the peaks disappeared. In fact, the spectra of porous alumina showed a broad band between 3600 cm^{-1} to 3200 cm^{-1} , assigned to the hydroxyl vibration of the hydrogen-bonded internal alumina groups. A sharp peak at about 1080 cm^{-1} to 1060 cm^{-1} may be attributed to Al-O-Al bonds in the spectrum of all supported complexes (Tunçel and Serin 2006; Uruş *et al.* 2010; Pan *et al.* 2013). Furthermore, the presence of weak bands around 3300 cm^{-1} in the $\text{NH}_2\text{-M}$ molecule were attributed to the N-H stretching of the amino groups. After grafting with alumina, the band due to N-H vibration disappeared with the formation of a new band at 1640 cm^{-1} , assigned to the vibration of C-N band, which indicated the participation of amino ligands in bonding with the metal ions (Salavati-Niasari *et al.* 2004; Ozdemir 2014). The peaks at 1636 cm^{-1} to 1594 cm^{-1} and 1366 cm^{-1} to 1352 cm^{-1} are the characteristic absorptions for asymmetric and symmetric stretching frequencies of $>\text{C}=\text{O}$ groups from L-tyrosine ligands (Salavati-Niasari *et al.* 2006; Görner and Wolff 2008). The peaks at about 496 cm^{-1} to 478 cm^{-1} and 598 cm^{-1} to 532 cm^{-1} are assigned to M-N and M-O stretching (Chandra and Kumar 2005; Salavati-Niasari *et al.* 2006; Karipcin and Kabalcilar 2007), respectively, in the complexes. The coordination modes of both N_{Amp} , N_{Tyr} , and O_{Tyr} atoms or O_{GA} atoms to metals are in agreement with the bands observed at 600 cm^{-1} to 480 cm^{-1} (Silva *et al.* 2011; Uruş *et al.* 2013; Ozdemir 2014).

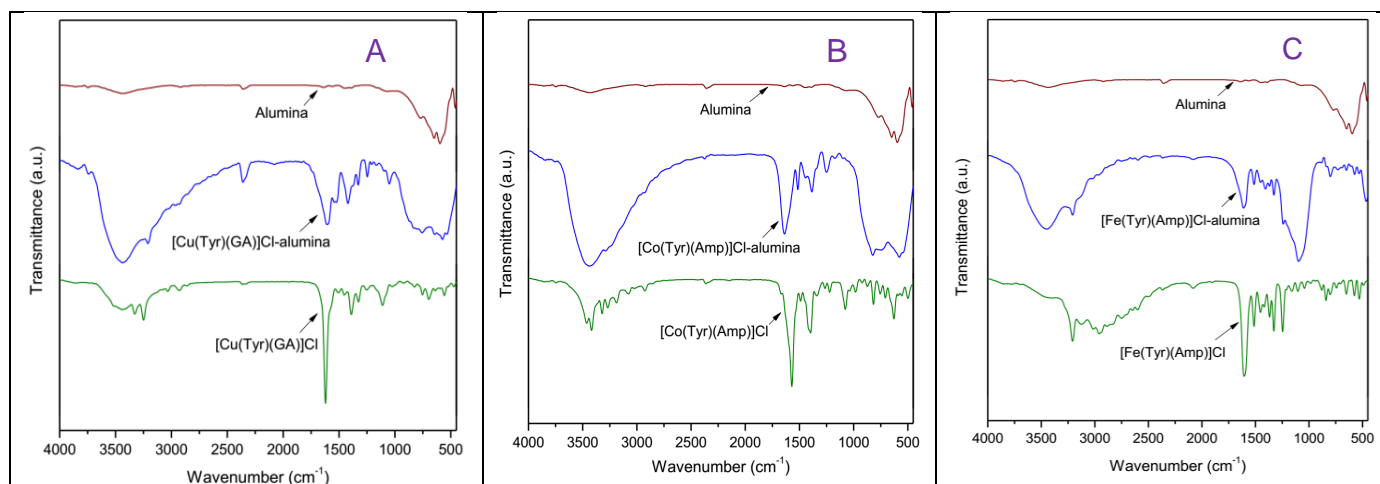


Fig. 3. The FTIR spectra of $[\text{Cu}(\text{Tyr})(\text{GA})]\text{Cl}$ and $[\text{Cu}(\text{Tyr})(\text{GA})]\text{Cl}$ -alumina (A), $[\text{Co}(\text{Tyr})(\text{Amp})]\text{Cl}$ and $[\text{Co}(\text{Tyr})(\text{Amp})]\text{Cl}$ -alumina (B), and $[\text{Fe}(\text{Tyr})(\text{Amp})]\text{Cl}$ and $[\text{Fe}(\text{Tyr})(\text{Amp})]\text{Cl}$ -alumina (C) in comparison with pure alumina support.

Elemental Analysis

The elemental analysis (carbon, hydrogen, and nitrogen) and metals were recorded by using a Yanaco CHN-corder-MT-5 at 550-950 °C after combustion and reduction process. Table 1 clearly shows the contents of various elements (C, H, and N) and metals of the three complexes. Here, Calcd. represented as calculated value.

Table 1. Elemental Analysis of Various Catalysts

Compound (Molecular Formula)	% Found (Calcd.)			
	C	H	N	Metal ^a
[Cu(Tyr)(GA)]Cl	42.91 (42.85)	3.38 (3.34)	3.15 (3.12)	14.25 (14.18)
[Co(Tyr)(Amp)]Cl	35.89 (35.86)	4.37 (4.34)	9.01 (8.97)	16.04 (15.99)
[Fe(Tyr)(Amp)]Cl	46.03 (45.99)	4.41 (4.38)	11.53 (11.49)	15.31 (15.28)

^aMetals detected are Cu, Co, Fe, and Cl.

Powder X-ray Diffraction Studies

The powder XRD patterns for [Cu(Tyr)(GA)]Cl and [Cu(Tyr)(GA)]Cl-alumina, [Co(Tyr)(Amp)]Cl and [Co(Tyr)(Amp)]Cl-alumina, and [Fe(Tyr)(Amp)]Cl and [Fe(Tyr)(Amp)]Cl-alumina are shown in Fig. 4. The observed interplanar d-spacing values were determined from the diffractogram of the complexes. Furthermore, the Miller indices h , k , and l values were attributed to each d-spacing along with 2θ angles. The results indicated that [Cu(Tyr)(GA)]Cl belonged to the monoclinic crystal system of space group C12, having unit cell parameters of $a = 23.54$, $b = 14.23$, and $c = 19.71$; and $\alpha = 90$, $\beta = 112$, and $\gamma = 90$ at the wavelength of 1.540598. For [Co(Tyr)(Amp)]Cl, results revealed the monoclinic crystal system of space group C12 of unit cell parameters, with $a = 10.03$, $b = 10.54$, $c = 14.96$; and $\alpha = 90$, $\beta = 110$, $\gamma = 90$. For complex [Fe(Tyr)(Amp)]Cl, space group P12 of unit cell parameters $a = 11.71$, $b = 16.30$, $c = 11.79$; and $\alpha = 90$, $\beta = 102$, $\gamma = 90$ at the wavelength of 1.540598 with maximum deviation of $2\theta = 0.025$, suggested that the metal complexes were crystalline (Li *et al.* 2016; Puškarić *et al.* 2016). However, metal complexes impregnated with alumina exhibited a sharp diffraction peak at around $2\theta = 2.5$, corresponding to the (1 0 0) reflection of native hexagonal mesoporous alumina lattices (Do Van *et al.* 2015). Furthermore, low intensity peaks of alumina phases were observed at ($2\theta = 15^\circ$ to 40°) due to (1 1 0), (2 0 0), and (2 0 0) reflections, which suggested that the metal complexes were uniformly incorporated within the alumina matrix. These results also imply that the metal complexes formed a hexagonally-packed mesoporous structure during the immobilization process (Didgikar *et al.* 2010; Payawan Jr. *et al.* 2010).

Thermogravimetric Analysis (TGA)

The thermal behaviour of ligand metal complexes and their corresponding alumina-tethered complexes were predicted by using thermogravimetric analysis (TGA) (Fig. 5). The TGA curves revealed that both homogeneous and heterogeneous metal complexes were thermally stable. In general, metal complexes had four endothermic peaks in the TGA diagrams. Physically adsorbed type water molecules on complexes were isolated at 50 °C to 90 °C with an endothermic peak in the TGA curves of complexes.

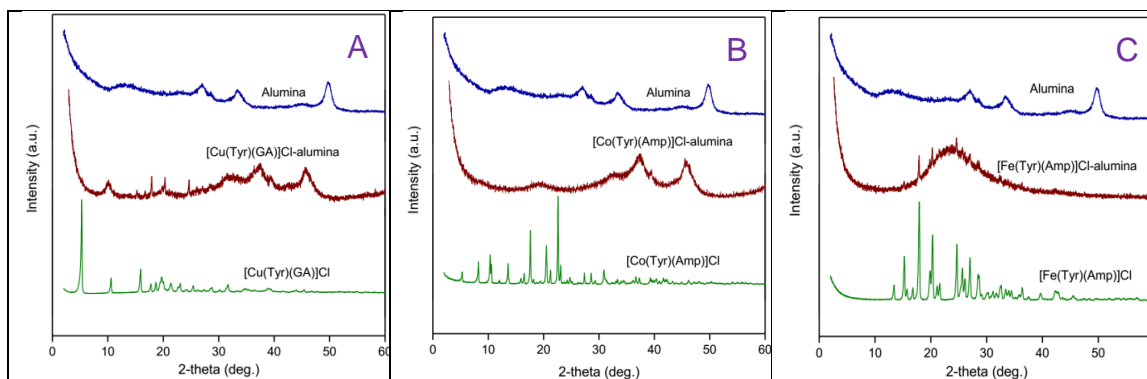


Fig. 4. The powder XRD patterns for (A) [Cu(Tyr)(GA)]Cl and [Cu(Tyr)(GA)]Cl-alumina; (B) [Co(Tyr)(Amp)]Cl and [Co(Tyr)(Amp)]Cl-alumina; and (C) [Fe(Tyr)(Amp)]Cl and [Fe(Tyr)(Amp)]Cl-alumina in comparison with pure alumina support

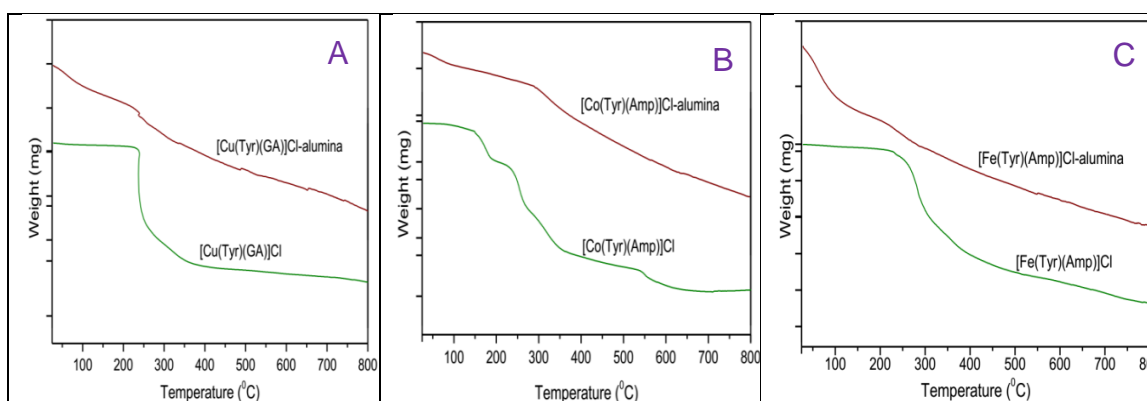


Fig. 5. TGA curves for (A) [Cu(Tyr)(GA)]Cl and [Cu(Tyr)(GA)]Cl-alumina; (B) [Co(Tyr)(Amp)]Cl and [Co(Tyr)(Amp)]Cl-alumina; and (C) [Fe(Tyr)(Amp)]Cl and [Fe(Tyr)(Amp)]Cl-alumina

The elimination of coordinated water and solvent molecules (Yang *et al.* 2011), from the metal complexes were determined at 100 °C to 240 °C. The peaks at about 260 °C to 350 °C were the degradations of coordinated chloride ions and one ligand group. The highest peaks were attributed between 400 °C to 800 °C when the elimination of another ligand group occurred and metal oxides finally formed. Generally, ligand groups with lower molecular masses were eliminated first, followed by the ligands with higher molecular masses, and the sequence of eliminating ligands were in the order of Amp>GA>Tyr (Dholariya *et al.* 2013). The same degradation patterns were also observed for all three impregnated complexes, where there was gradual weight loss followed by their corresponding complexes and finally the formation of metal oxide.

The alumina-supported mixed ligands do not allow a 1:2 ratio for metal-ligand complexation due to bulky structure of alumina. These proposed structures were according to the authors' previous reports and other literature that compared to FTIR, TGA, and other chemical or physical characterizations (Shchur *et al.* 2007; Tangestaninejad *et al.* 2009).

Scanning Electron Microscopy (SEM) Study

SEM imaging of the samples was performed to observe the surface morphology and physical structures before and after impregnation.

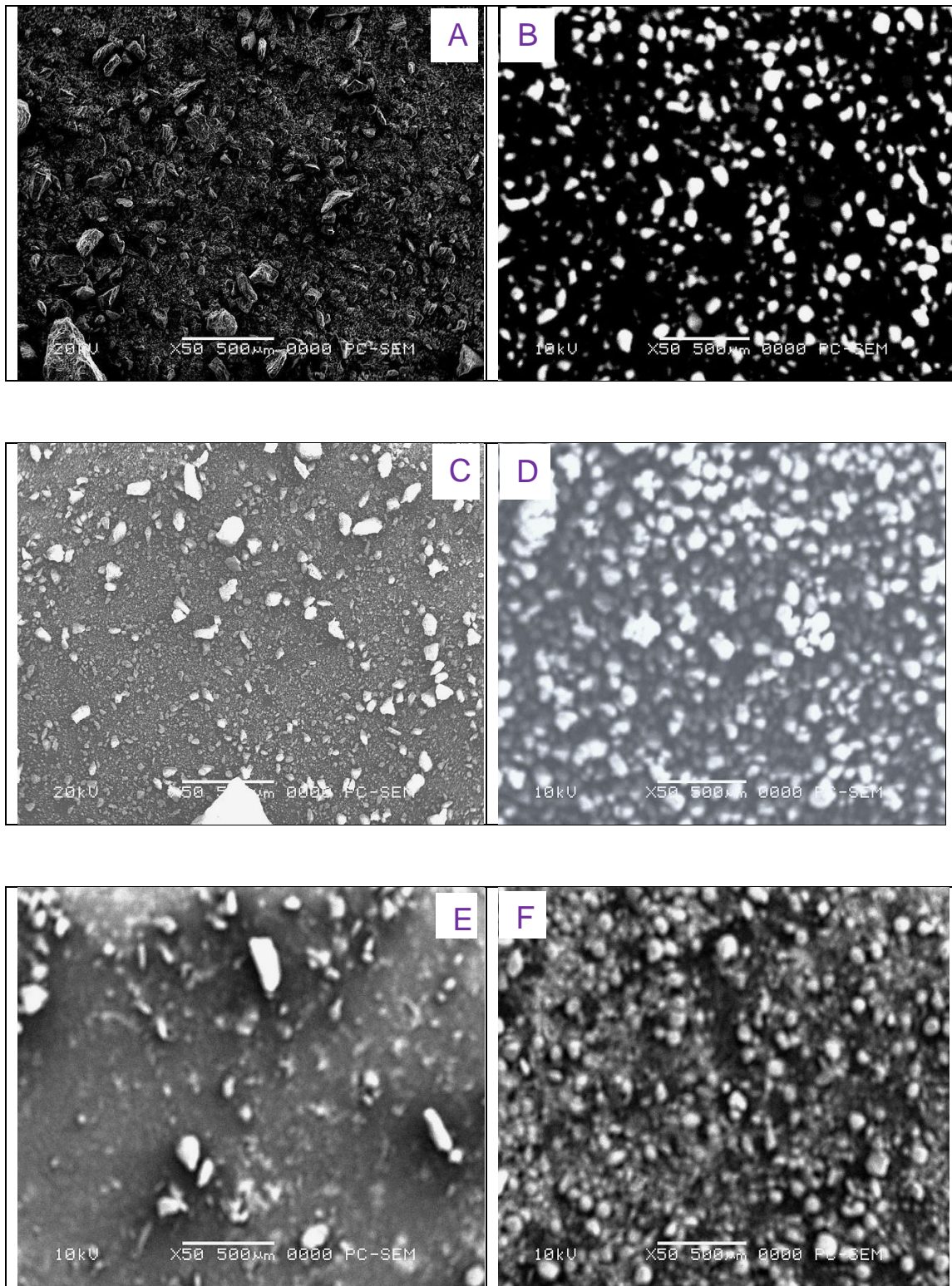


Fig. 6. The SEM images of (A) [Cu(Tyr)(GA)]Cl; (B) [Cu(Tyr)(GA)]Cl-alumina; (C) [Co(Tyr)(Amp)]Cl; (D) [Co(Tyr)(Amp)]Cl-alumina; (E) [Fe(Tyr)(Amp)]Cl; and (F) [Fe(Tyr)(Amp)]Cl-alumina at X50 magnification

The morphological differences between metal complexes and alumina-impregnated complexes in SEM images exhibited an important demonstration of loading of the complexes onto the alumina particles that formed clusters. These micrographs also showed a wide range of shapes and particle sizes after immobilization. Metal complexes diffused on the Al₂O₃ mesoporous channels that fitted perfectly with the pores. In general, the SEM micrograph displayed single-phase formation with well-defined, grain-like shapes which were particles sized in the range of 0.5 μm . Besides, different characteristic shapes of samples were identified, and these SEM images were quite different from other complexes. Additionally, the well-dispersed alumina-supported Cu(II), Co(II), and Fe(II) complexes exhibited good catalytic activity because they had large surface areas on the alumina particles and had cavities as an internal and external surface (Figs. 6(a), 6(b), and 6(c)) (Chaube *et al.* 2005; Salavati-Niasari *et al.* 2006; Islam *et al.* 2010). The EDX results further confirmed that metal ions were well-dispersed on the alumina-supported complexes (Fig. 7).

Energy Dispersive X-ray (EDX) Study

After immobilizing, the metal content of alumina-supported complexes was investigated by using energy dispersive X-ray spectroscopy (EDX). The EDX spectra at different points of the image (Fig. 7) confirm the presence of Cu, Co, and Fe in the surface alumina matrix. The atomic percentage of all elements of the complexes are given in Table 2. It is observed that the peaks corresponding to every elements were contributed in forming alumina tethered complexes.

Table 2. EDX Analysis of Various Catalysts

Compound	Atomic % of elements found				
	C	N	O	Al	Metal ^a
[Cu(Tyr)(GA)]Cl-alumina	18.41	0.92	51.24	29.03	0.39
[Co(Tyr)(Amp)]Cl-alumina	42.01	2.93	36.04	14.49	4.52
[Fe(Tyr)(Amp)]Cl-alumina	23.03	1.40	47.84	27.38	0.34

^aMetals are Cu, Co, and Fe, respectively.

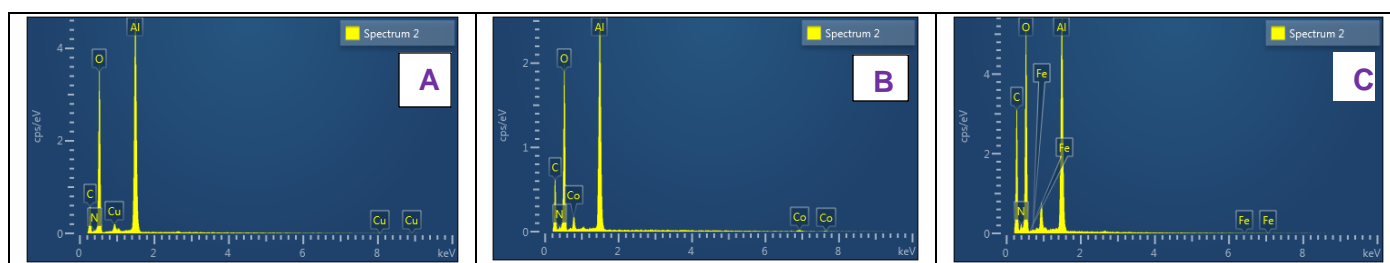


Fig. 7. EDX spectra of [Cu(Tyr)(GA)]Cl-alumina (A), [Co(Tyr)(Amp)]Cl-alumina (B), and [Fe(Tyr)(Amp)]Cl-alumina (C)

Catalytic Activity Study

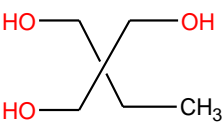
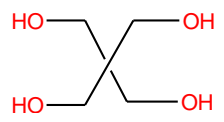
Esterification

The catalytic performances of the complexes were determined *via* esterification reactions of levulinic acid (LA) with two polyols, which were trimethylolpropane (TMP) and pentaerythritol (PE) (Table 3). Before investigating the activity of complexes, preliminary studies using sulfuric acid as a liquid acid catalyst were conducted to estimate

the range of reaction parameters (*i.e.*, reaction time, catalyst loading, and polyols to LA molar ratios). The molar ratio of LA to polyol was selected according to the stoichiometric ratio for the esterification reaction, where molar ratio of LA:TMP was 3:1 and the molar ratio of LA:PE is 4:1. The reaction temperature was optimized at 115 °C and 125 °C for TMP and PE esterification based on the ester yield and selectivity. A reaction duration of 2 h and catalyst loading of 2 wt.% with respect to LA were also optimized for all the complexes.

For all three complexes, the esterification of LA with TMP gave higher yields compared to PE. The trimethylolpropane had three (-OH) groups, resulting in LA-mono, LA-di, and LA-tri esters. On the other hand, pentaerythritol had four alcoholic groups and was less active, probably due to bulkiness of the molecule and higher melting point (533 K), so no tetra-ester product (Kotwal *et al.* 2013) was detected in this study. To compare the catalytic performances of these catalysts, similar reactions were conducted using H₂SO₄ as a catalyst (Ji *et al.* 2015), and observed alumina-tethered complexes (Table 4) had more potential than H₂SO₄ as the selectivity was higher for di- and tri- esters.

Table 3. Esterification of Levulinic Acid with (TMP) and (PE) over Cu(II), Co(II), and Fe(II) Complexes, H₂SO₄ and without Catalyst

Polyols	Catalysts	Ester yield (%) ^b		
		Mono	Di	Tri
Trimethylolpropane ^a 	[Cu(Tyr)(GA)]Cl	57.24	7.31	11.17
	[Co(Tyr)(Amp)]Cl	58.97	10.24	4.14
	[Fe(Tyr)(Amp)]Cl	48.24	7.41	4.92
	H ₂ SO ₄	51.00	15.0	1.50
	Blank experiment	14.86	2.00	0.85
Pentaerythritol ^{a,c} 	[Cu(Tyr)(GA)]Cl	49.30	10.14	5.58
	[Co(Tyr)(Amp)]Cl	50.13	8.88	3.07
	[Fe(Tyr)(Amp)]Cl	46.22	10.15	2.03
	H ₂ SO ₄	50.00	13.00	0.70
	Blank experiment	8.78	2.40	0.70

^aReaction conditions: Catalyst loading = 2% w/w of LA; LA: TMP= 3:1 at 115 °C, LA: PE= 4:1 at 125 °C; reaction time = 2 h

^bCalculated using Equation 1

^cNo tetra-ester product was detected for PE

Table 4. Esterification of Levulinic Acid with (TMP) and (PE) over Alumina-Supported Cu(II), Co(II), and Fe(II) Complex Catalysts

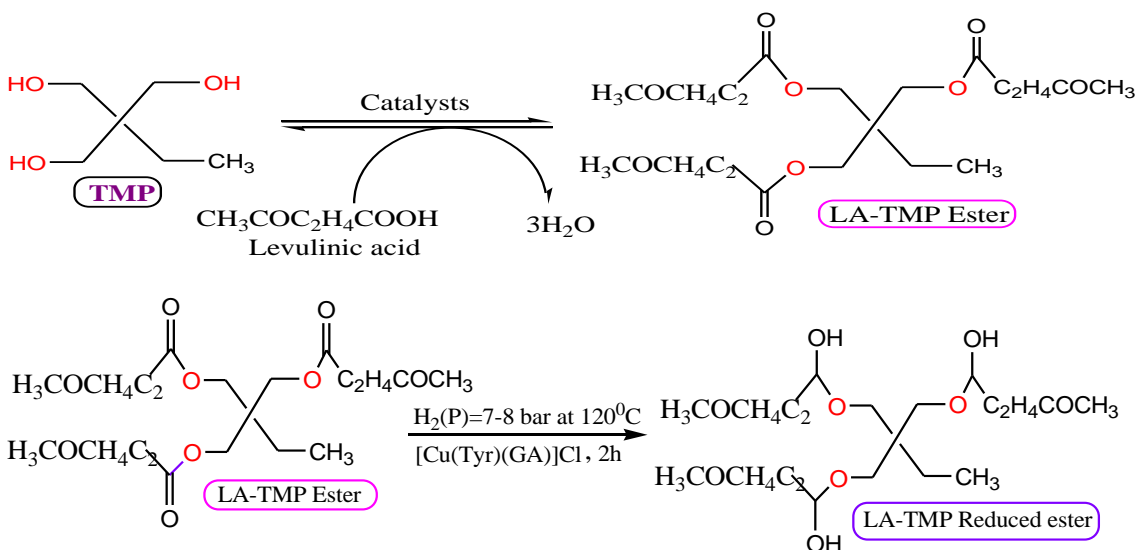
Polyols	Catalysts	Ester Yield (%) ^b		
		Mono	Di	Tri
TMP ^a	[Cu(Tyr)(GA)]Cl-alumina	33.89	33.00	8.83
	[Co(Tyr)(Amp)Cl]-alumina	16.51	60.14	5.05
	[Fe(Tyr)(Amp)]Cl-alumina	21.55	47.14	3.24
PE ^{a,c}	[Cu(Tyr)(GA)]Cl-alumina	31.28	28.23	4.23
	[Co(Tyr)(Amp)]Cl-alumina	23.89	41.83	5.08
	[Fe(Tyr)(Amp)]Cl-alumina	31.55	25.71	3.81

^aReaction conditions: Catalyst loading = 2% w/w of LA; LA: TMP= 3:1 at 115 °C, LA: PE= 4:1 at 125 °C, reaction time = 2 h (reflux condition)

^bCalculated using Equation 1

^cNo tetra-ester product was detected for PE

The present study also revealed that the ligand metal complexes impregnated with alumina were highly active for esterification of LA with TMP and PE, producing significant amounts of levulinate-di and levulinate-tri esters compared to their metal complexes. This might possibly have been complete immobilization of metal complexes onto alumina support which produced more Lewis acidic sites, and therefore produced more LA-di and LA-tri esters. As is known, no research paper is available yet for the esterification reaction of LA with TMP and PE over these complexes as catalyst. Currently, Masood *et al.* (2012) explained the suitability of heterogeneous Ca-methoxide catalyst to these chemical reactions. However, efficient purification methods are still essential as there is a tendency of metallic soap formation with catalyst to the fatty acids. Thus, impregnated complex catalysts in this study were highly active and selective for lubricant base oil production.

**Fig. 8.** Proposed synthetic route of LA-TMP ester and LA-TMP reduced ester, respectively

Catalytic activity *via* esterification revealed that the most active homogenous catalyst was [Cu(Tyr)(GA)]Cl, which yielded 75.72% TMP-LA ester and 65.02% PE-LA ester. Among the homogeneous complexes, Cu complex exhibited the highest activity with a majority of LA-tri esters. The most active alumina-supported metal complex was [Co(Tyr)(Amp)]Cl-alumina, which yielded 81.70% TMP-LA and 70.80% PE-LA ester. Among the supported complexes, Co complex after impregnation with alumina support generate more acidic sites, which favoured for the LA-di and LA-tri ester products. The mechanism for synthesizing esters and reduced esters (Figs. 8 and 9) is proposed.

Hydrogenation of Esters

Two active catalysts, [Cu(Tyr)(GA)]Cl and [Co(Tyr)(Amp)]Cl-alumina, were further investigated for the *in situ* hydrogenation of levulinate esters at 120 °C to 130 °C and 7 bar to 8 bar H₂ pressure in a closed reactor in the absence of air. The activity and selectivity of catalytic hydrogenation of LA-TMP and LA-PE esters to corresponding reduced esters over [Cu(Tyr)(GA)]Cl and [Co(Tyr)(Amp)]Cl-alumina catalysts is shown in Table 5. According to the esterification-hydrogenation reaction stoichiometry, one mol TMP/PE reacted with three/four mol LA, producing corresponding esters and reduced esters, respectively. Of the two cases, the authors used five mol LA (excess of polyol) with one mol TMP and PE, for completeness of the reaction in order to obtain maximum ester yield with highest selectivity.

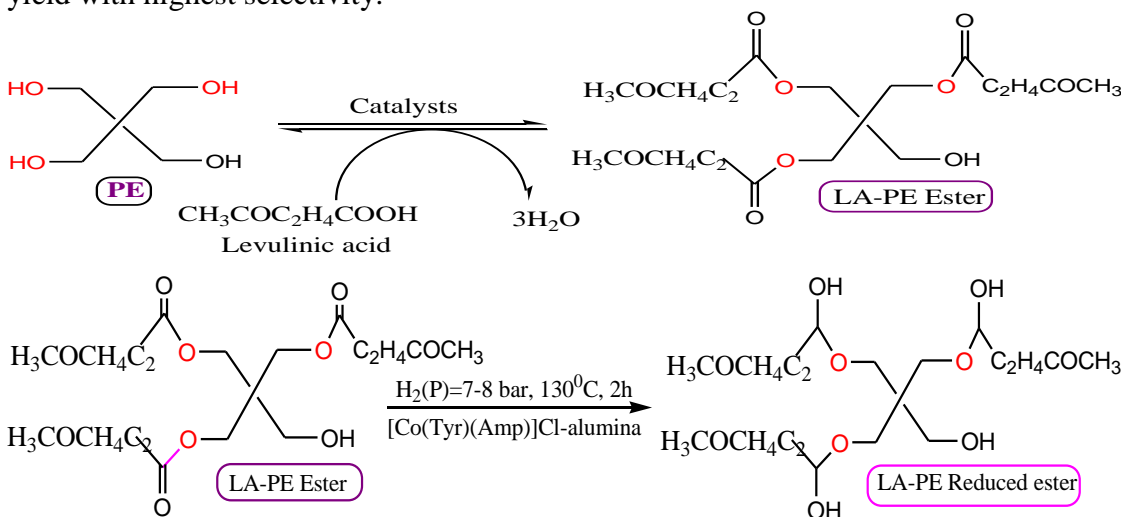


Fig. 9. Proposed synthetic route of LA-PE ester and LA-PE reduced ester, respectively

Table 5. Comparison by Yield of Ester and Reduced Ester Product after Esterification-Hydrogenation of LA with TMP and PE

Polyol	Catalyst	Reaction type	Reduced ester yield (%)		
			Mono	Di	Tri
TMP	[Cu(Tyr)(GA)]Cl	Esterification ^a	14.65	39.90	13.25
TMP	[Cu(Tyr)(GA)]Cl	Hydrogenation ^b	11.62	34.52	12.38
PE	[Co(Tyr)(Amp)]Cl-alumina	Esterification ^a	15.09	38.07	9.50
PE	[Co(Tyr)(Amp)]Cl-alumina	Hydrogenation ^b	13.45	35.52	8.58

^aReaction conditions: Catalyst loading = 2% w/w of LA; LA: TMP= 5:1 at 115 °C, LA: PE= 5:1 at 125 °C; reaction time = 2 h, product =ester (reflux condition)

^bReaction conditions: Catalyst loading = 2% w/w of LA; LA: TMP= 5:1 at 115 °C, LA: PE= 5:1 at 125 °C; reaction time= 2 h, H₂(P)= 7 bar to 8 bar, T= 120 °C for LA-TMP ester, and T= 130 °C for LA-PE ester with stirring speed 120 rpm to 130 rpm, product= reduced ester

Results from the experiment indicated that the significant amounts of LA-TMP and LA-PE esters were reduced after hydrogenation reaction. The reduction of LA-TMP and LA-PE esters was also confirmed by the analysis of IR spectra. GC-MS analysis revealed 58.52% reduced ester was isolated in the case of [Cu(Tyr)(GA)]Cl catalyst, whereas it was reduced by 57.55% for [Co(Tyr)(Amp)]Cl-alumina. Herein, [Co(Tyr)(Amp)]Cl-alumina was an efficient catalyst for the hydrogenation of LA-PE ester to corresponding reduced ester.

Chemical Modification of Levulinate Ester *via* Hydrogenation

Based on the results, hydrogenation of the levulinate ester was able to enhance its property as a biolubricant. Reduction of the ketone group from the levulinate chain can be carried out by employing H₂ at elevated temperature and pressure with the aid of a catalyst. Such modification significantly reduced side reactions such as polymerization, which can happen with the elevated working temperature of lubricating systems. Compared to the commercial vegetable oil-based biolubricants which are unsaturated, hydrogenized polyol esters enhanced fluid lubrication, boundary lubrication, and extreme pressure lubrication.

Catalyst Regeneration and Product Purification

The authors employed homogeneous as well as heterogeneous catalysts in the esterification-hydrogenation reaction. Results revealed that heterogeneous catalysts rendered higher activity compared to the corresponding homogeneous analogues. The higher yield was due to the availability of sufficient acidic sites in/on the cavities of immobilized complexes, which produced higher esters and hydrogenated esters, respectively.

The products containing di- and tri-esters were highly viscous and were resistant to separation of the catalyst. The heterogeneous catalyst could be separated *via* a repeated centrifugation method, from which the liquid product at the upper layer was collected. The process had to be repeated at least 3 times due to the high viscosity of product, in order to ensure maximum recovery of the product. The catalyst was then recovered by washing with methanol and water mixture, centrifuged, and vacuum-dried.

The homogeneous catalyst can be separated from the product *via* washing the product with cold methanol. The product was then heated at the low temperature of 65 °C to evaporate the methanol, while the metal complexes were recovered *via* recrystallization. Unfortunately, a reusability test was not carried out due to poor recoverability of the metal complexes.

Overall, results indicated that the selectivity of ester products contained significant amounts of monoester, which can be used for lower working temperature conditions in the petroleum industry as fuels and lubricants, as well as in cosmetic and food industries (Jackson 2003).

IR Spectra Analysis for Hydrogenated Esters (Reduced Esters)

Figures 10(a) and 10(b) represented the IR spectra for the ester product and hydrogenated product in comparison with LA for TMP ester and PE ester, respectively. Pure LA showed four characteristic bands in IR region: for C-H stretching at 2860 cm⁻¹ (s), C=O stretching at 1708 cm⁻¹ (s), C=O bending at 1170 cm⁻¹ (s), and O-H stretching for carboxylic group at 3300 cm⁻¹ to 2800 cm⁻¹ (b).

After esterification with TMP, LA-TMP ester experienced a shift to a higher wavenumber for C-H vibration at 2880 cm^{-1} (w), C=O bending at 1180 cm^{-1} (w), and C=O stretching at 1725 cm^{-1} (w) (Arbain and Salimon 2011). The disappearance of O-H stretch indicated that the carboxylic acid group was converted into ester form. After hydrogenation, the C=O stretching vibration appears at 1735 cm^{-1} , shifted to a 10 cm^{-1} higher wavenumber, indicated that C=O bond was likely converted into a C-O bond (Chakraborty *et al.* 2014).

After esterification with PE, LA-PE ester exhibited characteristic bands to higher wavenumber, therefore, for C-H stretching at 2890 cm^{-1} (w), C=O stretching at 1730 cm^{-1} (w), and C=O bending at 1185 cm^{-1} (w). After hydrogenation, the C=O experienced a little shift about 9 cm^{-1} to a higher wavenumber at 1739 cm^{-1} , represented that C=O bond was likely converted into C-O bond.

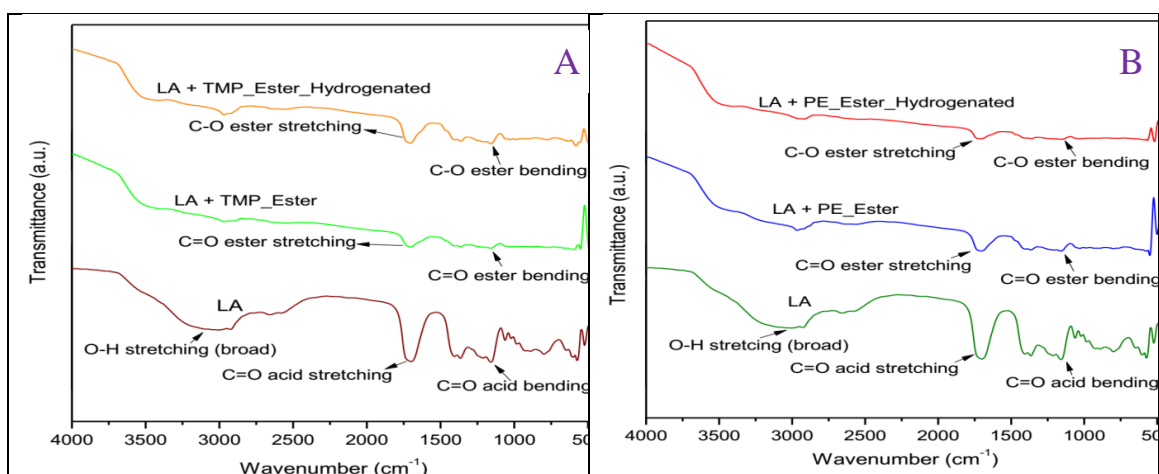


Fig. 10. IR spectra of (a) LA, LA + TMP ester, and hydrogenated LA + TMP ester; and (b) LA, LA + PE ester, and hydrogenated LA + PE ester

CONCLUSIONS

1. The polyol esters (*i.e.*, LA-TMP and LA-PE ester) had been successfully synthesized using bio-oil model compounds with the aid of metal complexes and alumina-supported metal complex catalysts.
2. Biomass-derived bio-oil model compound (levulinic acid) was considered as acid feedstock where levulinic acid was found as a major composition that could be extracted from crude bio-oil through molecular distillation process.
3. The polyol based-ester synthesized from non-food feedstock *via* esterification and upgraded through hydrogenation process had potential application as lubricant base oil with the aid of blending and formulation method.
4. The catalytic performances of the synthesized catalysts were evaluated *via* esterification of levulinic acid with trimethylolpropane (TMP) and pentaerythritol (PE). Results revealed that the most active homogenous catalyst was $[\text{Cu}(\text{Tyr})(\text{GA})]\text{Cl}$, which yielded 75.72% TMP-LA ester and 65.02% PE-LA ester.
5. The most active alumina-supported metal complex was $[\text{Co}(\text{Tyr})(\text{Amp})]\text{Cl}$ -alumina,

which rendered 81.70% TMP-LA and 70.77% PE-LA ester, respectively.

6. The two catalysts were further examined for the hydrogenation of levulinate esters, and GC-MS analysis revealed 58.52% reduced ester was isolated in the case of [Cu(Tyr)(GA)]Cl catalyst and 57.55% for [Co(Tyr)(Amp)]Cl-alumina.

ACKNOWLEDGEMENTS

The authors acknowledge the financial support from Universiti Malaya (Grand Challenge (Innovative Technology (ITRC) (GC001B-14AET)), RU Geran (ST014-2017), and Postgraduate Research Grant (PPP, Project number: PG250-2016A).

REFERENCES CITED

- Abbott, G., Brooks, R., Rosenberg, E., Terwilliger, M., Ross, J. A., and Ichire, O. O. (2014). "Surface-bound ruthenium diimine organometallic complexes: Excited-state properties," *Organometallics* 33(10), 2467-2478. DOI: 10.1021/om401153x
- Adhikary, J., Banerjee, P., and Chattopadhyay, T. (2015). "Alumina-supported Mn(III) and Fe(III) complexes of tridentate Schiff base ligand having ONO-donor sites: Syntheses, characterization and olefin epoxidation study," *Indian J. Chem., Sect. A* 54, 1175-1182.
- Arashiba, K., Miyake, Y., and Nishibayashi, Y. (2011). "A molybdenum complex bearing PNP-type pincer ligands leads to the catalytic reduction of dinitrogen into ammonia," *Nat. Chem.* 3(2), 120-125. DOI: 10.1038/nchem.906
- Arbain, N. H., and Salimon, J. (2011). "The effects of various acid catalyst on the esterification of *Jatropha curcas* oil based trimethylolpropane ester as biolubricant base stock," *J. Chem.* 8(S1), S33-S40. DOI: 10.1155/2011/789374
- Bergbreiter, D. E., Osburn, P. L., and Frels, J. D. (2001). "Nonpolar polymers for metal sequestration and ligand and catalyst recovery in thermomorphic systems," *J. Am. Chem. Soc.* 123(44), 11105-11106. DOI: 10.1021/ja016853o
- Bridgwater, A. V. (2012). "Review of fast pyrolysis of biomass and product upgrading," *Biomass Bioenergy* 38, 68-94. DOI: 10.1016/j.biombioe.2011.01.048
- Castonguay, A., Beauchamp, A. L., and Zargarian, D. (2008). "Preparation and reactivities of PCP-type pincer complexes of nickel. Impact of different ligand skeletons and phosphine substituents," *Organometallics* 27(21), 5723-5732. DOI: 10.1021/om8005454
- Chakraborty, S., Krause, J. A., and Guan, H. (2009). "Hydrosilylation of aldehydes and ketones catalyzed by nickel PCP-pincer hydride complexes," *Organometallics* 28(2), 582-586. DOI: 10.1021/om800948f
- Chandra, S., and Kumar, U. (2005). "Spectral and magnetic studies on manganese(II), cobalt(II) and nickel(II) complexes with Schiff bases," *Spectrochim. Acta A* 61(1-2), 219-224. DOI: 10.1016/j.saa.2004.03.036
- Chase, P. A., Klein Gebbink, R. J., and van Koten, G. (2004). "Where organometallics and dendrimers merge: The incorporation of organometallic species into dendritic molecules," *J. Organomet. Chem.* 689(24), 4016-4054. DOI: 10.1016/j.jorganchem.2004.07.032

- Chakraborty, S., Dai, H., Bhattacharya, P., Fairweather, N. T., Gibson, M. S., Krause, J. A., & Guan, H. (2014). "Iron-based catalysts for the hydrogenation of esters to alcohols," *Journal of the American Chemical Society*, 136(22), 7869-7872. DOI: 10.1021/ja504034q
- Chaube, V., Shylesh, S., and Singh, A. (2005). "Synthesis, characterization and catalytic activity of Mn(III)- and Co(II)-salen complexes immobilized mesoporous alumina," *J. Mol. Catal. A: Chem.* 241(1-2), 79-87. DOI: 10.1016/j.molcata.2005.07.005
- Choi, J., Choliy, Y., Zhang, X., Emge, T. J., Krogh-Jespersen, K., and Goldman, A. S. (2009). "Cleavage of sp³ C-O bonds *via* oxidative addition of C-H bonds," *J. Am. Chem. Soc.* 131(43), 15627-15629. DOI: 10.1021/ja906930u
- Climent, M. J., Corma, A., and Iborra, S. (2014). "Conversion of biomass platform molecules into fuel additives and liquid hydrocarbon fuels," *Green Chem.* 16(2), 516-547. DOI: 10.1039/C3GC41492B
- del Pozo, C., Corma, A., Iglesias, M., and Sánchez, F. (2010). "Immobilization of (NHC) NN-pincer complexes on mesoporous MCM-41 support," *Organometallics* 29(20), 4491-4498. DOI: 10.1021/om1006352
- Dholariya, H. R., Patel, K. S., Patel, J. C., and Patel, K. D. (2013). "Dicoumarol complexes of Cu(II) based on 1,10-phenanthroline: Synthesis, x-ray diffraction studies, thermal behavior and biological evaluation," *Spectrochim. Acta A* 108, 319-328. DOI: 10.1016/j.saa.2012.09.096
- Didgikar, M. R., Roy, D., Gupte, S. P., Joshi, S. S., and Chaudhari, R. V. (2010). "Immobilized palladium nanoparticles catalyzed oxidative carbonylation of amines," *Ind. Eng. Chem. Res.* 49(3), 1027-1032. DOI: 10.1021/ie9007024
- Do Van, D., Hosokawa, T., Saito, M., Horiuchi, Y., and Matsuoka, M. (2015). "A heterogeneous mesoporous silica-supported cyclopentadienyl ruthenium(II) complex catalyst for selective hydrosilylation of 1-hexyne at room temperature," *Appl. Catal. A* 503, 203-208. DOI: 10.1016/j.apcata.2015.05.039
- El Khatib, S., Hanafi, S., Arief, M., and Al-Amrousi, E. (2015). "Hydrocracking of jojoba oil for green fuel production," *J. Pet. Sci. Technol.* 5(2), 59-69. DOI: 10.22078/jpst.2015.505
- Gallezot, P. (2012). "Conversion of biomass to selected chemical products," *Chem. Soc. Rev.* 41(4), 1538-1558. DOI: 10.1039/C1CS15147A
- Goldman, A. S., Roy, A. H., Huang, Z., Ahuja, R., Schinski, W., and Brookhart, M. (2006). "Catalytic alkane metathesis by tandem alkane dehydrogenation-olefin metathesis," *Science* 312(5771), 257-261. DOI: 10.1126/science.1123787
- Goni, M. A., Rosenberg, E., Gobetto, R., and Chierotti, M. (2017). "Dehydrogenative coupling of alcohols to esters on a silica polyamine composite by immobilized PNN and PONOP pincer complexes of ruthenium," *J. Organomet. Chem.* 845, 213-228. DOI: 10.1016/j.jorganchem.2017.05.036
- Görner, H., and Wolff, T. (2008). "Lewis-acid-catalyzed photodimerization of coumarins and *N*-methyl-2-quinolone," *Photochem. Photobiol.* 84(5), 1224-1230. DOI: 10.1111/j.1751-1097.2008.00339.x
- Huang, Z., Brookhart, M., Goldman, A. S., Kundu, S., Ray, A., Scott, S. L., and Vicente, B. C. (2009). "Highly active and recyclable heterogeneous iridium pincer catalysts for transfer dehydrogenation of alkanes," *Adv. Synth. Catal.* 351(1-2), 188-206. DOI: 10.1002/adsc.200800615
- Ieda, N., Mantri, K., Miyata, Y., Ozaki, A., Komura, K., and Sugi, Y. (2008). "Esterification of long-chain acids and alcohols catalyzed by ferric chloride

- hexahydrate," *Ind. Eng. Chem. Res.* 47(22), 8631-8638. DOI: 10.1021/ie800957b
- Islam, M., Mondal, P., Mondal, S., Mukherjee, S., Roy, A. S., Mubarak, M., and Paul, M. (2010). "Use of a new polymer anchored Cu(II) azo complex catalyst for the efficient liquid phase oxidation reactions," *J. Inorg. Organomet. Polym. Mater.* 20(1), 87-96. DOI: 10.1007/s10904-009-9310-8
- Jackson, G. (2003). "Process for manufacturing monoesters of polyhydroxylalcohols," U.S. Patent No. 6664404.
- Jana, T. K., Kumar, D. P., Pradhan, R., Dinda, S., Ghosh, P. N., Simonnet, C., Marrot, J., Imaz, I., Wattiaux, A., Sutter, J.-P., Secheresse, F., and Bhattacharyya, R. (2009). "Synthesis and structure of iron (III) and iron (II) complexes in S₄P₂ environment created by diethyldithiocarbamate and 1,2-bis (diphenylphosphino)ethane chelation: Investigation of the electronic structure of the complexes by Mössbauer and magnetic studies," *Inorg. Chim. Acta* 362(10), 3583-3594. DOI: 10.1016/j.ica.2009.04.007
- Ji, H., Wang, B., Zhang, X., and Tan, T. (2015). "Synthesis of levulinic acid-based polyol ester and its influence on tribological behavior as a potential lubricant," *RSC Adv.* 5(122), 100443-100451. DOI: 10.1039/C5RA14366G
- Jones, C. W., McKittrick, M. W., Nguyen, J. V., and Yu, K. (2005). "Design of silica-tethered metal complexes for polymerization catalysis," *Top. Catal.* 34(1-4), 67-76. DOI: 10.1007/s11244-005-3790-8
- Karakhanov, E., Maximov, A., Kardasheva, Y., Semernina, V., Zolotukhina, A., Ivanov, A., Abbott, G., Rosenberg, E., and Vinokurov, V. (2014). "Pd nanoparticles in dendrimers immobilized on silica-polyamine composites as catalysts for selective hydrogenation," *ACS Appl. Mater. Interfaces* 6(11), 8807-8816. DOI: 10.1021/am501528a
- Karipcin, F., and Kabalcilar, E. (2007). "Spectroscopic and thermal studies on solid complexes of 4-(2-pyridylazo) resorcinol with some transition metals," *Acta Chim. Slov.* 54(2), 242-247.
- Kotwal, M., Kumar, A., and Darbha, S. (2013). "Three-dimensional, mesoporous titanosilicates as catalysts for producing biodiesel and biolubricants," *J. Mol. Catal. A: Chem.* 377, 65-73. DOI: 10.1016/j.molcata.2013.04.029
- Li, D., Xue, J., Ma, J., and Tang, J. (2016). "Synthesis of Fe₂(MoO₄)₃/MoO₃ heterostructured microrods and photocatalytic performances," *New J. Chem.* 40(4), 3330-3335. DOI: 10.1039/C5NJ03227J
- Masood, H., Yunus, R., Choong, T. S., Rashid, U., and Yap, Y. H. T. (2012). "Synthesis and characterization of calcium methoxide as heterogeneous catalyst for trimethylolpropane esters conversion reaction," *Appl. Catal. A* 425-426, 184-190. DOI: 10.1016/j.apcata.2012.03.019
- Mehendale, N. C., Sietsma, J. R., de Jong, K. P., van Walree, C. A., Klein Gebbink, R. J., and van Koten, G. (2007). "PCP- and SCS-pincer palladium complexes immobilized on mesoporous silica: Application in C-C bond formation reactions," *Adv. Synth. Catal.* 349(17-18), 2619-2630. DOI: 10.1002/adsc.200700330
- Morales-Morales, D., and Jensen, C. G. (2007). *The Chemistry of Pincer Compounds*, Elsevier, Amsterdam, The Netherlands.
- Müller, G., Klinga, M., Leskelä, M., and Rieger, B. (2002). "Iron and cobalt complexes of a series of tridentate P, N, P ligands—Synthesis, characterization, and application in ethene polymerization reactions," *Z. Anorg. Allg. Chem.* 628(13), 2839-2846. DOI: 10.1002/1521-3749(200213)628:13<2839::AID-ZAAC2839>3.0.CO;2-9
- Nandiwale, K. Y., and Bokade, V. V. (2016). "Optimization by Box–Behnken

- experimental design for synthesis of *n*-hexyl levulinate biolubricant over hierarchical H-ZSM-5: An effort towards agricultural waste minimization," *Process Saf. Environ. Prot.* 99, 159-166. DOI: 10.1016/j.psep.2015.11.003
- Nandiwale, K. Y., Yadava, S. K., and Bokade, V. V. (2014). "Production of octyl levulinate biolubricant over modified H-ZSM-5: Optimization by response surface methodology," *J. Energ. Chem.* 23(4), 535-541. DOI: 10.1016/S2095-4956(14)60182-0
- Oliveira, B. L., and da Silva, V. T. (2014). "Sulfonated carbon nanotubes as catalysts for the conversion of levulinic acid into ethyl levulinate," *Catal. Today* 234, 257-263. DOI: 10.1016/j.cattod.2013.11.028
- Ozdemir, M. (2014). "Catalytic activities of novel silica-supported multifunctional Schiff base ligand & metal complexes under microwave irradiation," *Inorg. Chim. Acta*, 421, 1-9. DOI: 10.1016/j.ica.2014.05.024
- Pan, H., Wang, J., Chen, L., Su, G., Cui, J., Meng, D., and Wu, X. (2013). "Preparation of sulfated alumina supported on mesoporous MCM-41 silica and its application in esterification," *Catal. Commun.* 35, 27-31. DOI: 10.1016/j.catcom.2013.02.007
- Payawan Jr., L., Damasco, J. A., and Sy Piecco, K. (2010). "Transesterification of oil extract from locally-cultivated *Jatropha curcas* using a heterogeneous base catalyst and determination of its properties as a viable biodiesel," *Philipp. J. Sci.* 139(1), 105-116.
- Puškarić, A., Halasz, I., Gredičak, M., Palčić, A., and Bronić, J. (2016). "Synthesis and structure characterization of zinc and cadmium dipeptide coordination polymers," *New J. Chem.* 40(5), 4252-4257. DOI: 10.1039/C5NJ03001C
- Salavati-Niasari, M., and Banitaba, S. (2003). "Alumina-supported Mn(II), Co(II), Ni(II) and Cu(II) bis(2-hydroxyanil) acetylacetonate complexes as catalysts for the oxidation of cyclohexene with *tert*-butylhydroperoxide," *J. Mol. Catal. A: Chem.* 201(1-2), 43-54. DOI: 10.1016/S1381-1169(03)00128-6
- Salavati-Niasari, M., Elzami, M., Mansournia, M., and Hydarzadeh, S. (2004). "Alumina-supported vanadyl complexes as catalysts for the C-H bond activation of cyclohexene with *tert*-butylhydroperoxide," *J. Mol. Catal. A: Chem.* 221(1-2), 169-175. DOI: 10.1016/j.molcata.2004.07.007
- Salavati-Niasari, M., Hassani-Kabutarkhani, M., and Davar, F. (2006). "Alumina-supported Mn(II), Co(II), Ni(II) and Cu(II) *N,N*-bis(salicylidene)-2,2-dimethylpropane-1,3-diamine complexes: Synthesis, characterization and catalytic oxidation of cyclohexene with *tert*-butylhydroperoxide and hydrogen peroxide," *Catal. Commun.* 7(12), 955-962. DOI: 10.1016/j.catcom.2006.04.005
- Santoro, A., Kershaw Cook, L. J., Kulmaczewski, R., Barrett, S. A., Cespedes, O., and Halcrow, M. A. (2015). "Iron(II) complexes of tridentate indazolyipyridine ligands: Enhanced spin-crossover hysteresis and ligand-based fluorescence," *Inorg. Chem.* 54(2), 682-693. DOI: 10.1021/ic502726q
- Serrano-Ruiz, J. C., Luque, R., and Sepúlveda-Escribano, A. (2011). "Transformations of biomass-derived platform molecules: From high added-value chemicals to fuels via aqueous-phase processing," *Chem. Soc. Rev.* 40(11), 5266-5281. DOI: 10.1039/C1CS15131B

- Serrano-Ruiz, J. C., Pineda, A., Balu, A. M., Luque, R., Campelo, J. M., Romero, A. A., and Ramos-Fernández, J. M. (2012). "Catalytic transformations of biomass-derived acids into advanced biofuels," *Catal. Today* 195(1), 162-168. DOI: 10.1016/j.cattod.2012.01.009
- Shchur, I., Khudina, O., Burgart, Y. V., Saloutin, V., Grishina, M., and Potemkin, V. (2007). "Synthesis, structure, and complexing ability of fluoroalkyl-containing 2,2'-(biphenyl-4,4'-diyldihydrazono)bis(1,3-dicarbonyl) compounds," *Russ. J. Org. Chem.* 43(12), 1781-1787. DOI: 10.1134/S107042800712007X
- Silva, T. F., da Silva, M. F. G., Mishra, G. S., Martins, L. M., and Pombeiro, A. J. (2011). "Synthesis and structural characterization of iron complexes with 2,2,2-tris(1-pyrazolyl)ethanol ligands: Application in the peroxidative oxidation of cyclohexane under mild conditions," *J. Organomet. Chem.* 696(6), 1310-1318. DOI: 10.1016/j.jorganchem.2010.12.036
- Swennenhuis, B. H., Chen, R., van Leeuwen, P. W., de Vries, J. G., and Kamer, P. C. (2009). "Supported chiral monodentate ligands in rhodium-catalysed asymmetric hydrogenation and palladium-catalysed asymmetric allylic alkylation," *Eur. J. Org. Chem.* 2009(33), 5796-5803. DOI: 10.1002/ejoc.200900911
- Taha, M., Khan, I., and Coutinho, J. A. (2016). "Complexation and molecular modeling studies of europium(III)-gallic acid-amino acid complexes," *J. Inorg. Biochem.* 157, 25-33. DOI: 10.1016/j.jinorgbio.2016.01.017
- Tangestaninejad, S., Moghadam, M., Mirkhani, V., Mohammadpoor-Baltork, I., and Ghani, K. (2009). "Alkene epoxidation catalyzed by molybdenum supported on functionalized MCM-41 containing N-S chelating Schiff base ligand," *Catal. Commun.* 10(6), 853-858. DOI: 10.1016/j.catcom.2008.12.010
- Tunçel, M., and Serin, S. (2006). "Synthesis and characterization of new azo-linked Schiff bases and their cobalt(II), copper(II) and nickel(II) complexes," *Transition Met. Chem.* 31(6), 805-812. DOI: 10.1007/s11243-006-0074-5
- Uruş, S., Dolaz, M., and Tümer, M. (2010). "Synthesis and catalytic activities of silica-supported multifunctional azo-containing schiff base complexes with Cu(II), Co(II), Ni(II) and Mn(II)," *J. Inorg. Organomet. Polym. Mater.* 20(4), 706-713. DOI: 10.1007/s10904-010-9394-1
- Uruş, S., Purtaş, S., Ceyhan, G., and Tümer, F. (2013). "Solid phase extraction of Pb(II), Cu(II), Cd(II) and Cr(III) with syringe technique using novel silica-supported bis(diazoimine) ligands," *Chem. Eng. J.* 220, 420-430. DOI: 10.1016/j.cej.2013.01.037
- Yang, Y., Zhang, Y., Hao, S., and Kan, Q. (2011). "Tethering of Cu(II), Co(II) and Fe(III) tetrahydro-salen and salen complexes onto amino-functionalized SBA-15: Effects of salen ligand hydrogenation on catalytic performances for aerobic epoxidation of styrene," *Chem. Eng. J.* 171(3), 1356-1366.
- Yi Lian, C.-L., Voon, L. H., and Abd Hamid, S. B. (2017). "Conversion of oleic acid model compound to biolubricant base oil using Al₂O₃ supported metal oxide catalyst," *Malay. J. Catal.* 2(2), 46-52.
- Yin, A., Guo, X., Dai, W.-L., and Fan, K. (2009). "The nature of active copper species in Cu-HMS catalyst for hydrogenation of dimethyl oxalate to ethylene glycol: New insights on the synergetic effect between Cu⁰ and Cu⁺," *J. Phys. Chem. C*, 113(25), 11003-11013. DOI: 10.1021/jp902688b

Zhang, B., Lin, L., Zhuang, J., Liu, Y., Peng, L., and Jiang, L. (2010). "Hydrogenation of ethyl acetate to ethanol over Ni-based catalysts obtained from Ni/Al hydrotalcite-like compounds," *Molecules* 15(8), 5139-5152. DOI: 10.3390/molecules15085139

Article submitted: March 10, 2018; Peer review completed: April 30, 2018; Revised version received and accepted: May 17, 2018; Published: June 4, 2018.

DOI: 10.15376/biores.13.3.5512-5533